

# Enhancement of the Fluorescence Quenching Efficiency of DPPH<sup>•</sup> on Colloidal Nanocrystalline Quantum Dots in Aqueous Micelles

Tuanjai Noipa · Surangkhan Martwiset ·  
Nutthaya Butwong · Thawatchai Tuntulani ·  
Wittaya Ngeontae

Received: 24 January 2011 / Accepted: 2 May 2011 / Published online: 15 May 2011  
© Springer Science+Business Media, LLC 2011

**Abstract** Luminescent CdS quantum dots capped with thioglycolic acid (CdS-TGA QDs) were demonstrated to serve as a fluorescence probe for a model organic radical, 2,2-diphenyl-1-picrylhydrazyl radical (DPPH<sup>•</sup>), employing the quenching of the CdS-TGA QDs emission signal by the radical. Under the optimum conditions, the quenching efficiency of DPPH<sup>•</sup> on CdS-TGA QDs was proportional to the concentration of DPPH<sup>•</sup>, following Stern-Volmer relationship. Different types of surfactants (cationic, anionic and neutral surfactants) were introduced to CdS-TGA QDs in order to increase the detection sensitivity. The fluorescence intensity of CdS-TGA QDs was greatly enhanced by cationic and neutral surfactants. Moreover, the quenching efficiency of DPPH<sup>•</sup> on the QDs in the presence of micelles was remarkably ca. 13 times higher than that in the system without micelles. Effects of pH and concentration of surfactants on the fluorescence quenching of CdS-TGA QDs were investigated. Electron spin resonance (ESR) spectroscopy was also used to monitor the DPPH radical species in CdS-TGA QDs mixtures with and without micelles. Fluorescence quenching mechanisms of CdS-TGA QDs by DPPH<sup>•</sup> in the presence and in the absence of CTAB were proposed.

**Keywords** Cadmium sulfide · Quantum dots · Micelle · DPPH radical · Fluorescence quenching

T. Noipa · S. Martwiset · N. Butwong · W. Ngeontae (✉)  
Department of Chemistry and Center for Innovation in Chemistry,  
Faculty of Science, Khon Kaen University,  
Khon Kaen 40002, Thailand  
e-mail: wittayange@kku.ac.th

T. Tuntulani  
Department of Chemistry, Faculty of Science,  
Chulalongkorn University,  
Bangkok 10330, Thailand

## Introduction

Free radicals are generally very reactive molecules possessing an unpaired electron. Interestingly, they can be continuously produced in cells either via a metabolism as by-products or a leakage from mitochondrial respiration. Radicals are also related to DNA damages, lipid peroxidation which causes aging and various diseases, and biological processes such as the oxidation of hemoglobin and phagocytosis of bacteria by leukocytes [1, 2]. Several methods including electron paramagnetic resonance (EPR) spectroscopy [3, 4], ultraviolet-visible (UV-vis) [5, 6] and fluorescence spectrophotometry [7–9] have been used to detect free radicals. Among these techniques, fluorescence spectrophotometry is the most promising tool due to its intrinsically high sensitivity.

Use of nanocrystalline QDs as a highly sensitive fluorescent probe for detecting organic radicals has recently attracted chemists' attention. However, the fluorescence quenching of QDs by organic radicals is not well understood. The sensing approach is based on intermolecular interactions, i.e. electrostatic or hydrogen bonding interactions between a organic capping on nanocrystalline QDs and an organic radical. Strong interactions between organic radicals and QDs are expected to improve the sensitivity of the sensors for chemical and biological applications.

A study by Scaiano and co-workers showed that the luminescence of trioctylphosphine oxide capped CdSe QDs could be quenched by nitroxyl free radicals in toluene solution, and the quenching was extremely non-linear and dependent on the nanoparticle size [10]. Recently, Braslau and co-workers further explored and showed that fluorescence quenching efficiency depended on the distance between nitroxide radical and the QDs surface [11]. Five nitroxide

radical derivatives were used in the study, and were monitored by EPR spectroscopy and fluorescence spectrophotometry. The fluorescence intensity of QDs could be restored by converting the nitroxide moiety to ethoxylamine or hydroxylamine. The same group also demonstrated the use of CdSe QDs for the detection of carbon centered free radicals generated from azo-bis-isobutyronitrile (AIBN) [12]. The sensing approach was based on the recovery of the fluorescence intensity of the CdSe QDs-4-amino-2,2,6,6-tetramethylpiperidine-1-oxyl (4-amino TEMPO) system.

Since the fluorescence intensity of QDs highly depends on the surface states of the QDs, one would expect that interactions between free radicals and the surface of QDs may influence the efficiency of the electron-hole recombination process, leading to luminescence change of the QDs [13]. Sanz-Medel and co-workers have reported that high signal stability of QDs can be achieved when a surfactant was introduced [14].

In this work, we investigated interactions between thioglycolic capped CdS QDs (CdS-TGA QDs) and free radicals using DPPH free radical (DPPH<sup>•</sup>) as a model molecule. A feasibility of the CdS-TGA QDs quenching by DPPH<sup>•</sup> was examined. The CdS-TGA QDs were further modified by an addition of various surfactants, and their fluorescence quenching sensitivity was studied. Possible mechanisms of interactions between the QDs and DPPH<sup>•</sup> in the absence and in the presence of surfactants were also discussed.

## Experimental Section

### Chemicals

All chemicals were of analytical grade and used without further purification. All aqueous solutions were prepared from deionized water with the specific resistivity of 18.2 M $\Omega$  cm from RiO<sub>5</sub><sup>TM</sup> Type I Simplicity 185 (Millipore water). Thioglycolic acid (TGA) and 2,2-diphenyl-1-picrylhydrazyl (DPPH<sup>•</sup>) were purchased from Sigma-Aldrich. Cadmium chloride (CdCl<sub>2</sub>·H<sub>2</sub>O) was obtained from Riedel-deHaen. Sodium sulfide (Na<sub>2</sub>S·H<sub>2</sub>O) and sodium dodecyl sulphate (SDS) were received from BDH. Triton-X 100, cetyltrimethylammonium bromide (CTAB), dodecyltrimethylammonium bromide (DTAB) and trimethyltetradecylammonium bromide (TTAB) were purchased from Fluka. Glacial acetic acid and sodium acetate were obtained from Carlo Erba. Methanol (MeOH) was purchased from Lab Scan.

### Instrumentation

Fluorescence spectra were recorded using a RF-5301PC spectrofluorophotometer (Shimadzu). The slit widths used

for the excitation and emission were 5 nm. Absorption spectra of samples were acquired on an Agilent HP 8453 spectrophotometer. pH measurements were made with a Thermo Orion pH meter. An H-7650 Transmission Electron Microscope (TEM) (Hitachi High-Technology Corporation, Japan) operating at 100 kV was used to collect TEM images of the colloidal CdS-TGA QDs. Electron spin resonance (ESR) measurements were recorded using a JEOL JES-RE2X ESR spectrometer. Measurement conditions were adjusted with central field of 336.8 mT, modulation frequency at 100 kHz, modulation amplitude of 1.25 $\times$ 100, microwave power at 1.0 mW, microwave frequency at 9.45 GHz and temperature set to 273 K.

### Procedure

#### *Synthesis of TGA Capped CdS Quantum Dots*

TGA-capped CdS QDs were prepared using a procedure from the literature with modification [15]. A solution of CdCl<sub>2</sub>·H<sub>2</sub>O (18.75 mmol) in 200 mL of deionized water was stirred at room temperature for 30 min. Thioglycolic acid (2.60 mL) was then added to the solution. The reaction mixture was stirred under nitrogen for at least 30 min. The pH was adjusted to 10.5 by a dropwise addition of 1 M NaOH aqueous solution with constant stirring. In a different flask, Na<sub>2</sub>S·H<sub>2</sub>O (20.56 mmol) was dissolved in 10 mL of deionized water. The Na<sub>2</sub>S solution was subsequently added into the reaction mixture under nitrogen. After refluxing at 75 °C under nitrogen for 1 h, a bright yellow-green colloid was obtained. Colloidal quantum dots were stored at room temperature. No precipitation was observed over a 1-month period.

#### *General Procedures for Fluorescence Quenching*

To study a fluorescence quenching of the prepared TGA-capped CdS QDs by DPPH<sup>•</sup>, the following general procedures were carried out. DPPH<sup>•</sup> was dissolved in methanol. The solution was then diluted with deionized water to provide desired DPPH<sup>•</sup> concentrations. To a 100- $\mu$ L colloidal nanocrystals of CdS-TGA QDs, various concentrations of DPPH<sup>•</sup> solution were added. The 0.1 M acetate buffer with a pH of 4.6 was added to the mixture to make a final volume of 10.00 mL. The mixture was then incubated at room temperature for 5 min. The relative fluorescence intensity was measured at  $\lambda_{em}/\lambda_{ex}=510/370$  nm. To study pH and incubation time effects on the fluorescence intensity of CdS-TGA QDs, the pH of 0.1 M acetate buffer was varied from 4.5 to 7.5 prior to addition to the mixture of CdS-TGA QDs and DPPH<sup>•</sup>. The incubation time was varied from 0.5 to 30 min.

### Introduction of a Surfactant

Influences of surfactant types and surfactant tail lengths on the fluorescence intensity of CdS-TGA QDs were studied by addition of the desired amount of surfactant solutions to the CdS-TGA QDs solution in a 10.00 mL volumetric flask. After the mixture was diluted to the mark with 0.1 M acetate buffer pH 4.6, the fluorescence intensity was measured at  $\lambda_{\text{ex}}$  370 nm.

The influence of cetyltrimethylammonium bromide (CTAB) concentration on the fluorescence intensity of the TGA-capped CdS QDs was investigated by addition of different amount of CTAB aqueous solution to the CdS-TGA QDs solution. The mixture was diluted with 0.1 M acetate buffer pH 4.6 to make a final volume of 10.00 mL. The mixture was incubated for 5 min prior to measurements of absorption and emission spectra at  $\lambda_{\text{ex}}$  370 nm.

### ESR Measurements

In order to study the DPPH form after mixing with CdS-TGA QDs in acetate buffer and CTAB solution, the following procedures were conducted. The DPPH<sup>•</sup> solution was added into CdS-TGA QDs solution. The 0.1 M acetate buffer pH 4.6 was added to obtain a final volume of 10.00 mL. The mixture was incubated for 5 min prior to the measurement. For the CTAB micellar system, the same procedures were performed with addition of appropriate concentrations of CTAB.

## Results and Discussion

### CdS-TGA QDs

#### Characteristics of CdS-TGA QDs

The absorption and emission spectra of the thioglycolic acid-capped CdS QDs were shown in Fig. 1. The synthesized QDs possessed an absorption maximum of the first excitonic peak at 375 nm and displayed an emission maximum at 510 nm upon the excitation at 370 nm. Particle sizes of the synthesized CdS-TGA QDs were also measured by a transmission electron microscope. Figure 2 showed the TEM image of the CdS-TGA QDs. The nanoparticles were generally spherical with diameters of  $27.3 \pm 4.0$  nm.

#### pH Dependence

It has been reported that pH is one of the major parameters that affect the fluorescence intensity of the QDs [16, 17]. In this study, the influence of pH in the range of 4.5 to 7.5 on the fluorescence intensity of CdS-TGA QDs was

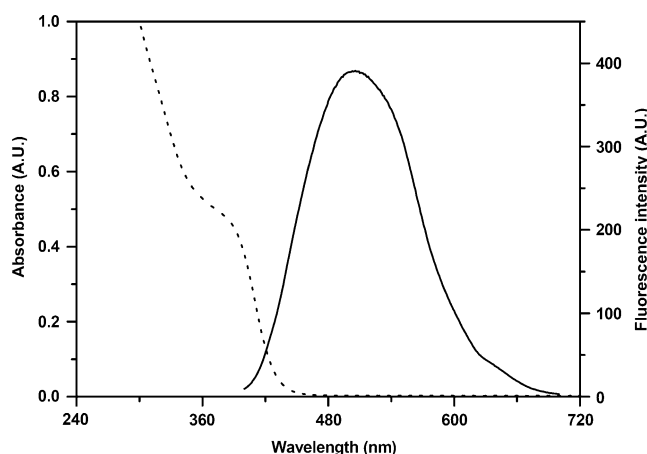


**Fig. 1** Absorbance spectrum (---) and fluorescence emission spectrum (—) of 0.5 mM CdS-TGA QDs in 0.1 M acetate buffer pH 4.6 ( $\lambda_{\text{em}}/\lambda_{\text{ex}}=510/370$  nm)

investigated. The pHs of the solution were varied by adjusting the pH of 0.1 M acetic-acetate buffer. The results were shown in Fig. 3A. It was found that the pH of the solution affected the fluorescence intensity of the synthesized CdS-TGA QDs. The fluorescence intensity of CdS-TGA QDs increased initially and decreased afterward. The maximum fluorescence intensity was obtained in the pH range of 5.0–5.5.

### CdS-TGA QDs in the Presence of DPPH<sup>•</sup>

#### Effect of pH on Fluorescence Intensity

The effect of pH on interactions between CdS-TGA QDs and DPPH<sup>•</sup> was also studied. The low fluorescence intensity at low pHs (shown in Fig. 3A) could be attributed to a dissociation of the Cd<sup>2+</sup>-TGA-QDs from the protonation of the surface binding thiolates [18]. A plot of pH vs.

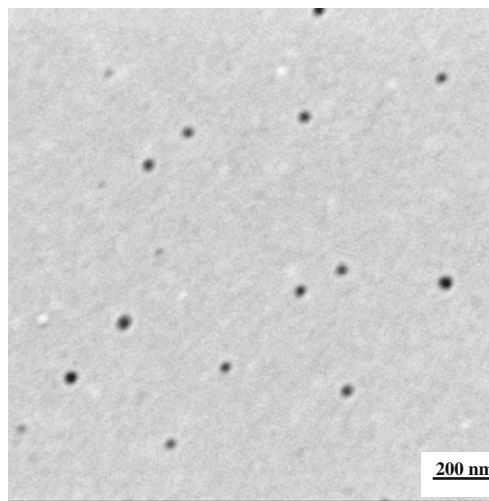
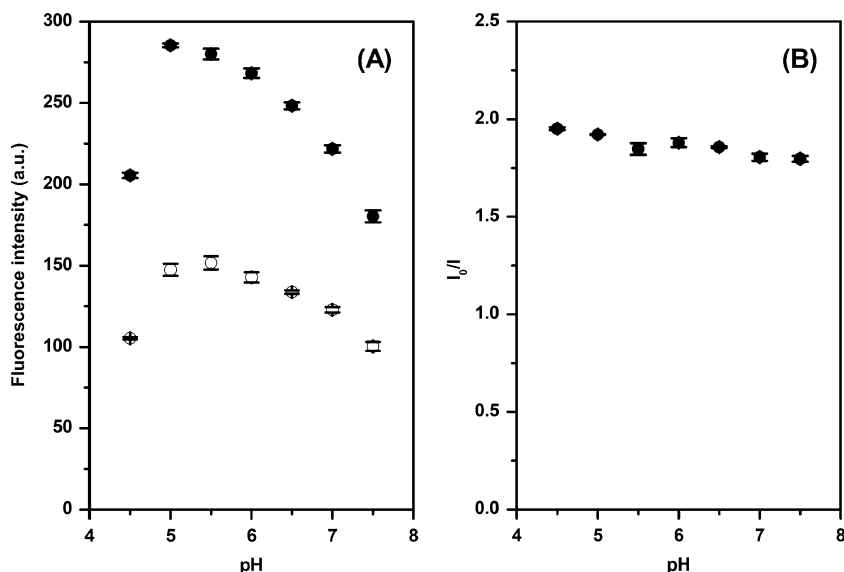


**Fig. 2** TEM image of the synthesized CdS-TGA QDs

**Fig. 3** (A and B) Effect of pH on the fluorescence intensity (•: QDs, ○: QDs-DPPH<sup>•</sup>). Concentrations: CdS-TGA QDs 0.5 mM; DPPH<sup>•</sup> 0.05 mM ( $I_0$  and  $I$  are the fluorescence intensities of CdS-TGA QDs in the absence and in the presence of DPPH<sup>•</sup>, respectively)



relative fluorescence quenching ( $I_0/I$ ), where  $I_0$  and  $I$  are the fluorescence intensities of the QDs in the absence and presence of DPPH<sup>•</sup>, respectively, was shown in Fig. 3B. A constant relative quenching over a wide pH range was observed. Since high fluorescence intensity and sensitivity were obtained at pH 4.6, this pH was chosen as an optimized condition in further investigations.

*Fluorescence Quenching by DPPH<sup>•</sup>*

The influence of DPPH<sup>•</sup> on the fluorescence intensity of CdS-TGA QDs was studied. The emission spectra of CdS-TGA QDs and that of CdS-TGA QDs titrated with DPPH<sup>•</sup>, recorded in a pH 4.6 acetate buffer, were shown in Fig. 4A. The fluorescence intensity decreased gradually with increasing DPPH<sup>•</sup> concentration. No discernible change in

shapes of the fluorescence spectra was observed upon quenching; however, a slight blue shift at high DPPH<sup>•</sup> concentrations was seen. To illustrate the quenching effect of DPPH<sup>•</sup> concentration on the fluorescence intensity of CdS-TGA QDs, Stern-Volmer’s equation was applied. The Stern-Volmer quenching behavior was driven by the collision between the luminescent molecule and the quencher. This model is classified as the dynamic quenching [19]. The Stern-Volmer relationship is given in the following equation.

$$\frac{I_0}{I} = 1 + K_{SV}[Q] \tag{1}$$

where  $I_0$  and  $I$  are the fluorescence intensities of CdS-TGA QDs in the absence and in the presence of DPPH<sup>•</sup>,

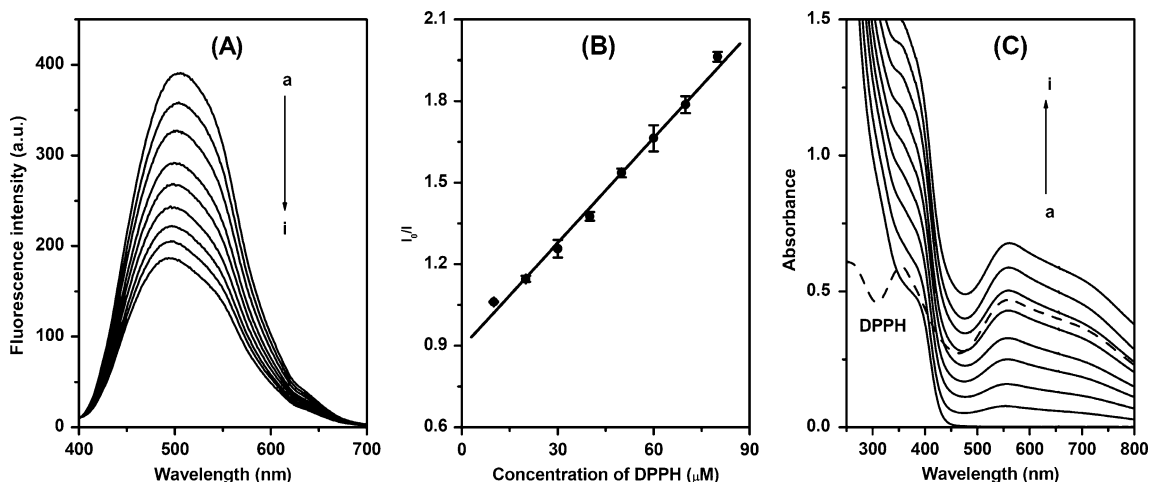


**Fig. 4** (A) Fluorescence emission spectra and (C) absorbance spectra of 0.5 mM CdS-TGA QDs in the presence of various concentrations of DPPH<sup>•</sup> in 0.1 M acetate buffer pH 4.6 (a: absence of DPPH<sup>•</sup>, b–i:

10, 20, 30, 40, 50, 60, 70 and 80  $\mu\text{M}$ ). Absorption spectrum of 0.05 mM DPPH<sup>•</sup> in 0.1 M acetate buffer pH 4.6 (----). (B) The corresponding linear plot by Stern–Volmer analysis

respectively.  $K_{SV}$  is the Stern-Volmer quenching constant which is related to the quenching efficiency and  $[Q]$  is the concentration of DPPH $^{\bullet}$ . As shown in Fig. 4B, a linear relationship between the ratio of  $I_0$  to  $I$  and DPPH $^{\bullet}$  concentration was observed in the range of 10–80  $\mu\text{M}$  with a  $K_{SV}$  of  $1.4 \times 10^4 \text{ M}^{-1}$ . The remarkably large  $K_{SV}$  value suggested a high quenching efficiency of DPPH free radical and that CdS-TGA QDs can possibly be used as a sensitive probe for organic radical sensors.

#### *Possible Mechanisms of Interactions Between CdS-TGA QDs and DPPH $^{\bullet}$*

While organic solvents have been generally used to precipitate out QDs [20–22], a small volume of methanol is needed to disperse DPPH radicals in water. In order to understand the interactions between CdS-TGA QDs and DPPH $^{\bullet}$ , the influence of organic solvents on the fluorescence intensity of CdS-TGA QDs was considered. Three common organic solvents used in QDs precipitation, methanol, ethanol and propanol, were chosen. The results showed that the fluorescence intensity of CdS-TGA QDs was quenched when such solvent was added. The relative fluorescence intensity ( $I_0/I$ ) of the QDs increased with increasing solvent volume. Similar to previous reports [20–22], this increment is thought to be a result from the precipitation of CdS-TGA QDs. Interestingly, when the solvent volume used was lower than 2% v/v, no significant change in the fluorescence intensity was observed. Therefore, the volume of organic solvent was kept below 2%v/v in further experiments in order to avoid the organic solvent effect that leads to the fluorescence quenching of CdS-TGA QDs in the presence of DPPH $^{\bullet}$ .

Besides a change in fluorescence intensity, the interactions between CdS-TGA QDs and DPPH $^{\bullet}$  were also observed in an absorption spectrum. UV-Visible spectrophotometry provided useful information, especially types of the present species in the solution based on the spectrum pattern and the maximum absorption wavelength ( $\lambda_{\text{max}}$ ). The information of changes of DPPH $^{\bullet}$  and its related species in solution (not fluorescence active) was also measured parallel by spectrophotometry. As shown in Fig. 4C, in the pH 4.6 buffer, the absorption characteristic peak of DPPH $^{\bullet}$  appeared at 560 nm, and CdS-TGA QDs showed an absorption maximum of the first excitation at 375 nm. When DPPH $^{\bullet}$  was added to the CdS-TGA QDs solution, the absorption spectrum showed a combination pattern of CdS-TGA QDs and DPPH $^{\bullet}$ . As the DPPH $^{\bullet}$  concentration was increased, the absorption intensity of the combination pattern increased, whereas the corresponding fluorescence intensity of CdS-TGA QDs showed the opposite trend, Fig. 4A. These results indicate that DPPH $^{\bullet}$  existed as free radical and caused the fluorescence quenching of CdS-TGA QDs.

In this system, DPPH $^{\bullet}$  may interact with the thioglycolic moieties via a strong charge–charge induced interaction. The interaction could provide a close distance between the radical and the QDs, assisting the electron transfer process. When the QDs were excited by photons, a separation between electron ( $e^-$ ) and hole ( $h^+$ ) from the valence band will occur. The electron will consequently shift to the conducting band. Due to the effective distance between the adsorbed DPPH $^{\bullet}$  and the QDs surface, the electron from the conducting band is able to transfer to the singly occupied molecular orbital (SOMO) of DPPH $^{\bullet}$  following by the relaxation to the original state (valence band).

In order to confirm the presence of the free radical form of DPPH, ESR experiment was carried out with the same solution composition as in the fluorescence study. The ESR results were shown in Fig. 5A. It could be seen that the CdS-TGA QDs in the buffer solution were not active in ESR. The QDs solution became active after the addition of DPPH $^{\bullet}$  since a sharp and intense peak, corresponding to the suspended solid DPPH $^{\bullet}$ , was detected [23]. This observation confirmed that DPPH existed in the free radical form after mixing with CdS-TGA QDs in the buffer solution.

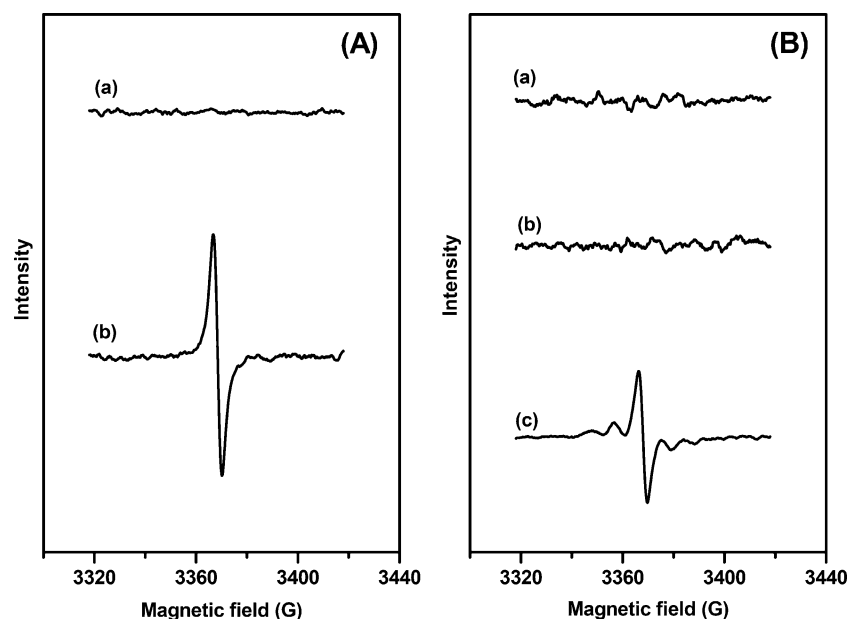
#### *Introduction of Surfactants*

We were interested in using the surfactant sphere to act as a nano-vessel for CdS-TGA QDs and the radical. Due to different chemical environments, polarity and lipophilicity of the inside and outside of micelles are remarkably different. It is expected that chemical behaviors such as the rate of reaction and the solubility of the compound in the micellar system would be different from those in the bulk solution. Moreover, the electronic energy state which is stabilized by the surfactant tends to change in the excitation or relaxation process of the QDs and would result in increasing of the fluorescence intensity.

#### *Influence of Surfactant Types on the Fluorescence Intensity of CdS-TGA QDs*

Three types of surfactants, neutral (Triton X-100), anionic (SDS) and cationic (CTAB) surfactants in 0.1 M acetate buffer pH 4.6, were studied. The concentration of each surfactant used in this study was twice its critical micelle concentration (cmc): 0.48 mM Triton X-100, 18 mM SDS and 2 mM CTAB [24, 25]. The CdS-TGA QDs were mixed separately with the three surfactants and the fluorescence intensities were measured. The results were shown in Table 1. The fluorescence intensity of CdS-TGA QDs increased by 8.50% and 16.42% in the presence of CTAB and Triton X-100 micelles, respectively. On the other hand, in the presence of SDS, the fluorescence intensity decreased by 5.05%. The enhancement of the fluorescence intensity of

**Fig. 5** ESR spectra of 0.5 mM CdS-TGA QDs in the absence (a) and in the presence (b) of 0.04 mM DPPH<sup>•</sup> in (A) 0.1 M acetate buffer pH 4.6. (B) 10 mM CTAB in 0.1 M acetate buffer pH 4.6. ESR spectrum of 0.05 mM DPPH<sup>•</sup> in 2 mM CTAB in 0.1 M acetate buffer pH 4.6 (c)



CdS-TGA QDs in the presence of cationic and neutral surfactants may be due to a partial incorporation of CdS-TGA QDs into the surfactant micelle. The incorporation leads to a separation of CdS-TGA QDs from the bulk solution, which prevents an adsorption of other molecules on the surface of the QDs. Therefore, the excited electron from conducting band can be directly combined with  $h^+$  (at the valence band) without electron transfer to other molecules. Moreover, the concentration of the QDs inside the micelle is relatively higher than those in regular solution. In contrast, in the presence of SDS, the decrease in fluorescence intensity can be ascribed to the electrostatic repulsion between the negative charge on the surface of CdS-TGA QDs and the anionic head of SDS, which limits the incorporation of CdS-TGA QDs into the surfactant micelle.

In addition, the reactions between DPPH<sup>•</sup> and CdS-TGA QDs in the three surfactant micelles were also investigated in order to improve the fluorescence quenching sensitivity.

**Table 1** Effect of surfactant types and tail of cationic surfactant on the fluorescence intensity of CdS-TGA QDs and the fluorescence quenching by DPPH free radical

Surfactant	Change of fluorescence (%)	Fluorescence quenching by DPPH <sup>•</sup> ( $I_0/I$ )
Triton X-100	+16.42±0.58	1.11±0.01
SDS	-5.05±0.12	0.98±0.02
CTAB (C <sub>16</sub> )	+8.50±0.84	4.00±0.06
TTAB (C <sub>14</sub> )	+12.98±1.65	1.78±0.03
DTAB (C <sub>12</sub> )	+11.32±0.61	1.45±0.07

Experimental conditions: 0.48 mM Triton X-100, 18 mM SDS, 2 mM CTAB, 8 mM TTAB, 32 mM DTAB, 0.01 mM DPPH<sup>•</sup>, medium; 0.1 M acetate buffer pH 4.6

The concentration of DPPH<sup>•</sup> was fixed at 0.01 mM. The fluorescence quenching ability of DPPH<sup>•</sup> was represented in terms of relative fluorescence quenching ( $I_0/I$ ), where  $I_0$  and  $I$  are the fluorescence intensities of CdS-TGA QDs in the absence and in the presence of DPPH<sup>•</sup>, respectively, shown in Table 1. While a slight increase in fluorescence intensity ( $I_0/I < 1$ ) was observed when DPPH<sup>•</sup> was introduced to the SDS system, the intensities were dropped in the Triton X-100 and CTAB systems. A maximum quenching efficiency was observed in the presence of CTAB, suggesting that cationic surfactant (CTAB) was a suitable surfactant that could be used to increase the fluorescence quenching ability of DPPH<sup>•</sup>.

#### *Influence of Cationic Surfactant Tail on the Fluorescence Intensity of CdS-TGA QDs*

To further explore the role of the tail of cationic surfactants on the fluorescence intensity of CdS-TGA QDs, three cationic surfactants with different tail lengths, CTAB (C<sub>16</sub>), TTAB (C<sub>14</sub>) and DTAB (C<sub>12</sub>), were used in this study. The concentration of each surfactant was twice its cmc: 2 mM CTAB, 8 mM TTAB and 32 mM DTAB [24]. It was shown in Table 1 that the three surfactants could enhance the fluorescence intensity of CdS-TGA QDs, and the degrees of enhancement were similar, indicating that the tail length of the cationic surfactant did not affect the fluorescence intensity of CdS-TGA QDs.

Furthermore, the fluorescence quenching by DPPH<sup>•</sup> in the presence of the three cationic surfactants was also investigated. The relative fluorescence quenching ( $I_0/I$ ) in the three systems were shown in Table 1. The observed fluorescence quenching ability of DPPH<sup>•</sup> in the presence of

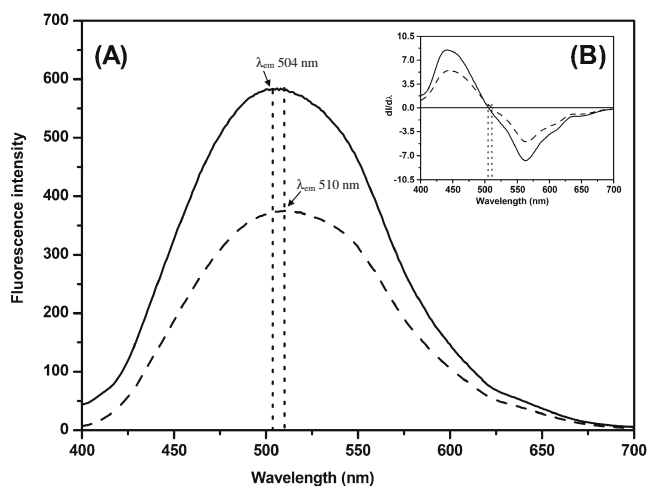


**Fig. 6** (A) Fluorescence emission spectra of 0.5 mM CdS-TGA QDs in the absence (---) and in the presence (—) of 10 mM CTAB in 0.1 M acetate buffer pH 4.6. (B) Inset: First derivative spectrum of 0.5 mM CdS-TGA QDs in the absence (---) and in the presence (—) of 10 mM CTAB in 0.1 M acetate buffer pH 4.6

CTAB micelles was higher than that in the presence of TTAB and DTAB micelles. This may be due to the larger size and more hydrophobicity of the micelles formed from CTAB, which has the longest tail among the three surfactants. Therefore, it is easier for DPPH<sup>•</sup> and CdS-TGA QDs to incorporate into CTAB, leading to higher concentrations of both DPPH<sup>•</sup> and CdS-TGA QDs inside the CTAB micelle.

*Effect of the Concentration of CTAB on Fluorescence Enhancement*

To further explore the role of CTAB in the enhancement of fluorescence intensity of CdS-TGA QDs, the effect of CTAB

concentration was studied. The concentrations of CTAB were varied from 0 to 50 mM. The fluorescence intensities of the resulting mixtures of CTAB and CdS-TGA QDs solutions were measured. When the CTAB concentrations were ≤10 mM, the fluorescence intensities of the modified QDs were enhanced, i.e.  $I/I_0 > 1.0$ . When the concentration was more than 10 mM, a drop in intensity was observed. The increment in fluorescence intensity of CdS-TGA QDs at CTAB concentrations below the cmc, 1.0 mM, is due to electrostatic interactions between positive charges of CTAB and negative charges of CdS-TGA QDs surface. These interactions suppress non-radiative recombination at surface vacancies [26]. The emission spectra of CdS-TGA QDs in the absence and in the presence of 10 mM CTAB micelle in 0.1 M acetate buffer pH 4.6 were shown in Fig. 6. The enhancement in fluorescence intensity observed could be attributed to the partial incorporation of CdS-TGA QDs into the hydrophobic core of CTAB micelle. The concentration of CTAB was chosen to be 10 mM to provide a maximum fluorescence enhancement in further investigations.

The hydrophilic CdS-TGA QDs can incorporate inside the hydrophobic core of the micelle due to electrostatic interactions between the negative charge on the surface of CdS-TGA QDs and the positive charge of surface of CTAB micelle. Therefore, the QDs may be located close to the positive charge of the CTAB micelle. This result is supported by the slight blue shift from 510 nm to 504 nm observed in the micellar system (Fig. 6). This shift could be a result of a transfer of CdS-TGA QDs from a polar environment of the bulk aqueous phase to a less polar environment of the micellar aggregates of CTAB [27].

The indirect evidence was the behavior of CdS-TGA QDs in the presence of anionic SDS micelle as shown in

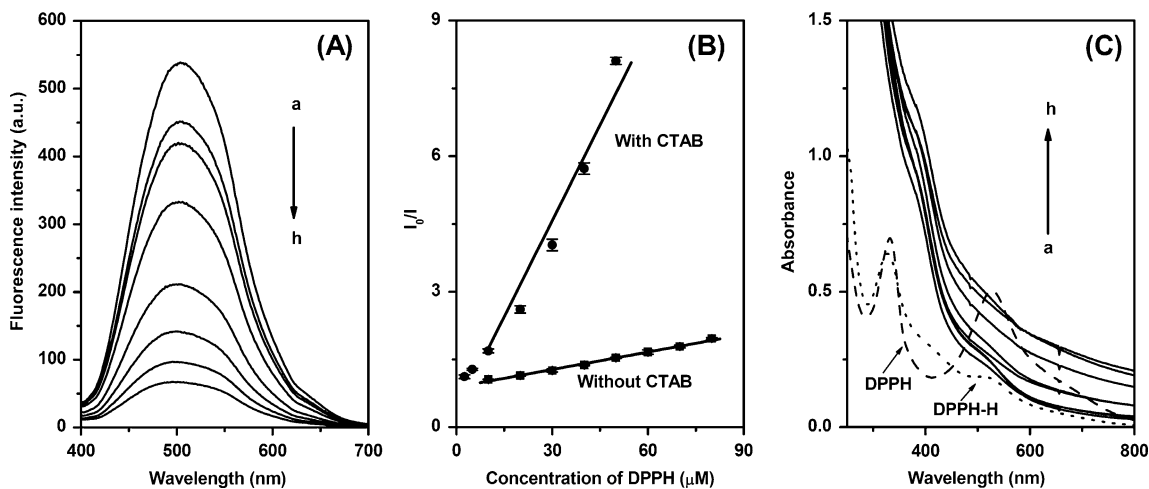


**Fig. 7** (A) Fluorescence emission spectra and (C) absorbance spectra of 0.5 mM CdS-TGA QDs in the presence of various concentrations of DPPH<sup>•</sup> in 10 mM CTAB in 0.1 M acetate buffer pH 4.6 (a: absence of DPPH<sup>•</sup>, b–h: 2.5, 5, 10, 20, 30, 40 and 50 μM). Absorption spectrum of 0.05 mM DPPH<sup>•</sup> in 10 mM CTAB in 0.1 M acetate buffer

pH 4.6 (---). Absorption of DPPH-H prepared from the mixing 0.05 mM DPPH<sup>•</sup> and 0.1 mM gallic acid in 10 mM CTAB in 0.1 M acetate buffer pH 4.6 (····). (B) Comparison of Stern–Volmer plots between the systems with CTAB (●) and without (■) CTAB

Table 1. These results suggested that the CdS-TGA QDs were not incorporated into the micelle of SDS due to the repulsion between the negative charge of SDS micelle and surface of CdS-TGA QDs. Therefore, the fluorescence intensity of the QDs was not increased. On the other hand, DPPH<sup>•</sup> is basically a hydrophobic molecule and tends to incorporate inside the hydrophobic core of the micelle.

#### *Possible Mechanisms of Fluorescence Quenching by an Assistance of CTAB*

It was shown in the previous section that the fluorescence intensity of CdS-TGA QDs could be enhanced in the presence of CTAB micelles. The effect of DPPH<sup>•</sup> on fluorescence intensity of CdS-TGA QDs in a micelle solution was then investigated. Figure 7A showed that the fluorescence intensity was dramatically quenched upon addition of DPPH<sup>•</sup>. The relative intensity was directly proportional to the concentration of DPPH<sup>•</sup>, agreeing with the Stern-Volmer relationship (Fig. 7B). The quenching constant,  $K_{SV}$ , was determined to be  $1.7 \times 10^5 \text{ M}^{-1}$ . This quenching constant is an order of magnitude higher than that from the system with no micelle mentioned earlier. A plot of DPPH<sup>•</sup> concentration vs. relative fluorescence intensity obtained from both systems in Fig. 7B clearly showed that in the presence of micelles, the quenching efficiency of DPPH<sup>•</sup> on CdS-TGA QDs was enhanced.

Interactions between DPPH<sup>•</sup> and CdS-TGA QDs in the micellar system were also investigated by UV-Visible spectrophotometry. The absorption spectra of CdS-TGA QDs in the presence of different concentrations of DPPH<sup>•</sup> and in the presence of micelles were shown in Fig. 7C. It could be seen that the purple color of DPPH<sup>•</sup> in the micellar solution exhibited the absorption peak at 528 nm. Upon the gradual addition of DPPH<sup>•</sup> to the CdS-TGA QDs solution, an absorption peak at 528 nm disappeared, whereas the corresponding intensity of the emission spectra of CdS-TGA QDs decreased with increasing DPPH<sup>•</sup> concentration (Fig. 7A). The disappearance of the absorption peak at 528 nm may be due to a change of DPPH<sup>•</sup> form to DPPH-H form [28, 29]. This change could be attributed to the donation of hydrogen atom from the capping molecule on the surface of CdS-TGA QDs to DPPH free radical which may occur inside the micellar hydrophobic sphere.

The disappearance of the radical form was also elucidated by ESR spectroscopy as shown in Fig. 5B. The mixtures of CTAB and CdS-TGA QDs in the presence and in the absence of DPPH<sup>•</sup> were not active in ESR. A combination pattern of solid and solution structures was observed when DPPH<sup>•</sup> was added to the CTAB solution in the absence of CdS-TGA QDs. This characteristic revealed that DPPH<sup>•</sup> was in the hydrophobic core of the micelle [30]. Therefore, this

implied that in the micelle system, the interactions between CdS-TGA QDs and DPPH<sup>•</sup> occurred inside the micelle. This result was remarkably different from that of the buffer solution system. The disappearance of the radical was a result from the H transfer from CdS-TGA QDs to DPPH<sup>•</sup> in CTAB media.

#### **Conclusion**

The feasibility of the water soluble thioglycolic acid-capped CdS quantum dot as a fluorescence probe for sensing a stable organic radical was developed. This sensor was based on the fluorescence quenching of DPPH free radical which interacted with CdS-TGA QDs. Under optimum conditions, the extent of fluorescence quenching of the modified QDs was linearly proportional to the concentration of DPPH<sup>•</sup>. The quenching behavior was described by Stern-Volmer relationship. The influences of surfactant types and surfactant tail length on the fluorescence intensity of CdS-TGA QDs were investigated. It was found that the fluorescence intensity could be enhanced through the incorporation of the QDs into the hydrophobic core of cationic (CTAB) and neutral (Triton-X) micelles. Two different forms of DPPH<sup>•</sup> after mixing with CdS-TGA QDs in the buffer solution and in the CTAB solution observed in ESR spectra suggested that the quenching mechanisms in the two solutions were different. In the buffer solution, the DPPH<sup>•</sup> can quench the fluorescence intensity of the CdS-TGA QDs and retains its radical form. However, the enhanced quenching efficiency of DPPH<sup>•</sup> on CdS-TGA QDs obtained in the presence of CTAB was due to H transfer to DPPH<sup>•</sup> to generate DPPH-H species. The knowledge from this work may lead to the development of a new approach for sensors in food and health cares.

**Acknowledgements** This research was financially supported by the Higher Education Research Promotion and National Research University Project of Thailand, Office of the Higher Education Commission, through the Advanced Functional Materials Cluster of Khon Kaen University, the Thailand Research Fund (RTA5380003) and the Center for Innovation in Chemistry (PERCH-CIC), Commission on Higher Education, Ministry of Education. T.N. is a Ph.D. student partially supported by Kasetsart University, Chalermphrakiat Sakon Nakhon Province Campus.

#### **References**

- Martinez-Cayuela M (1995) Oxygen free radicals and human disease. *Biochimie* 77:147–161
- Tang DC, Chen TW, Huang TP, Chen CL, Liu TY, Wei YH (2002) Increased oxidative damage to peripheral blood leukocyte DNA in chronic peritoneal patients. *J Am Soc Nephrol* 13:1321–1330
- Espinoza M, Olea-Azar C, Speisky H, Rodriguez J (2009) Determination of reactions between free radicals and selected Chilean wines and transition metals by ESR and UV-vis technique. *Spectrochim Acta A* 71:1638–1643



4. Yordanov ND, Rangelova K (2000) Quantitative electron paramagnetic resonance and spectrophotometric determination of the free radical 4-hydroxy-2,2,6,6-tetramethylpiperidinyloxy. *Spectrochim Acta A* 56:373–378
5. Souza LC, Araújo SMS, Imbroisi DO (2004) Determination of the free radical scavenging activity of dihydropyran-2,4-diones. *Bioorg Med Chem Lett* 14:5859–5861
6. Wang BS, Li BS, Zeng QX, Liu HX (2008) Antioxidant and free radical scavenging activities of pigments extracted from molasses alcohol wastewater. *Food Chem* 107:1198–1204
7. Scaiano JC, Aliaga C, Chrétién MN, Frenette M, Focsaneanu KS, Mikelsons L (2005) Fluorescence sensor applications as detectors for DNA damage, free radical formation, and in microlithography. *Pure Appl Chem* 77:1009–1018
8. Tang B, Zhang L, Hu JX, Li P, Zhang H, Zhao YX (2004) Indirect determination of superoxide anion radical in the plant of red sage based on vanillin-8-aminoquinoline with fluorescence. *Anal Chim Acta* 502:125–131
9. Yang X-F, Guo X-Q (2001) Study of nitroxide-linked naphthalene as a fluorescence probe for hydroxyl radicals. *Anal Chim Acta* 434:169–177
10. Laferrière M, Galian RE, Maurel V, Scaiano JC (2006) Non-linear effects in the quenching of fluorescent quantum dot by nitroxyl free radicals. *Chem Commun* 257–259
11. Tansakul C, Lilie E, Walter ED, Rivera F III, Wolcott A, Zhang JZ, Millhauser GL, Braslau R (2010) Distance-dependent fluorescence quenching and binding of CdSe quantum dots by functionalized nitroxide radicals. *J Phys Chem C* 114:7793–7805
12. Maurel V, Laferrière M, Billone P, Godin R, Scaiano JC (2006) Free radical sensor based on CdSe quantum dots with added 4-amino-2,2,6,6-tetramethylpiperidine oxide functionality. *J Phys Chem B* 110:16353–16358
13. Moore DE, Patel K (2001) Q-CdS Photoluminescence activation on Zn<sup>2+</sup> and Cd<sup>2+</sup> salt introduction. *Langmuir* 17:2541–2544
14. Fernández-Argüelles MT, Jin WJ, Costa-Fernández JM, Pereiro R, Sanz-Medel A (2005) Surface-modified CdSe quantum dots for the sensitive and selective determination of Cu(II) in aqueous solutions by luminescent measurements. *Anal Chim Acta* 549:20–25
15. Chen J, Zheng A, Gao Y, He C, Wu G, Chen Y, Kai X, Zhu C (2008) Functionalized CdS quantum dots-based luminescence probe for detection of heavy and transition metal ions in aqueous solution. *Spectrochim Acta A* 69:1044–1052
16. Cai Z-X, Yang H, Zhang Y, Yan X-P (2006) Preparation, characterization and evaluation of water-soluble L-cysteine-capped-CdS nanoparticles as fluorescence probe for detection of Hg(II) in aqueous solution. *Anal Chim Acta* 559:234–239
17. Skoog DA, Holler FJ, Nieman TA (1998) Principles of instrumental analysis. Saunders College, Philadelphia
18. Gao M, Kirstein S, Möhwald H, Rogach AL, Kornowski A, Eychmüller A, Weller H (1998) Strongly photoluminescent CdTe nanocrystals by proper surface modification. *J Phys Chem B* 102:8360–8363
19. Lakowicz JR (1999) Principles of fluorescence spectroscopy. Plenum Press, New York
20. Koneswaran M, Narayanaswamy R (2003) L-Cysteine-capped ZnS quantum dots based fluorescence sensor for Cu<sup>2+</sup> ion. *Sens Actuator B-Chemical* 139:104–109
21. Li H, Zhang Y, Wang X (2007) L-Carnitine capped quantum dots as luminescent probes for cadmium ions. *Sens Actuator B-Chemical* 127:593–597
22. Yuan J, Guo W, Yin J, Wang E (2009) Glutathione-capped CdTe quantum dots for the sensitive detection of glucose. *Talanta* 77:1858–1863
23. Chen C, Tang HR, Sutcliffe LH, Belton PS (2000) Green tea polyphenols react with 1,1-diphenyl-2-picrylhydrazyl free radicals in the bilayer of liposomes: direct evidence from electron spin resonance studies. *J Agric Food Chem* 48:5710–5714
24. Attwood D, Florence AT (1983) Surfactant systems. Chapman and Hall, London
25. Bohne C, Redmond RW, Scaiano JC (1991) Use of photophysical techniques in the study of organized assemblies. VCH, New York
26. Chena X, Donga Y, Fanb L, Yang D (2007) Fluorescence for the ultrasensitive detection of peptides with functionalized nano-ZnS. *Anal Chim Acta* 582:281–287
27. Sowmiya M, Tiwari AK, Saha SK (2010) Fluorescent probe studies of micropolarity, premicellar and micellar aggregation of non-ionic Brij surfactants. *J Colloid Interface Sci* 344:97–104
28. Brand-Williams W, Cuverlier ME, Berset C (1995) Use of a free radical method to evaluate antioxidant activity. *Lebensm Wiss Technol* 28:25–30
29. Matthäus B (2002) Antioxidant activity of extracts obtained from residues of different oilseeds. *J Agric Food Chem* 50:3444–3452
30. Noipa T, Srijaranai S, Tuntulani T, Ngeontae W (2011) New approach for evaluation of the antioxidant capacity based on scavenging DPPH free radical in micelle systems. *Food Res Int* 44:798–806